The Journal of Chemical Physics

A master equation simulation for the $^{\bullet}OH + CH_3OH$ reaction

Cite as: J. Chem. Phys. **150**, 084105 (2019); https://doi.org/10.1063/1.5081827
Submitted: 16 November 2018 . Accepted: 01 February 2019 . Published Online: 25 February 2019

Thanh Lam Nguyen, Branko Ruscic, and John F. Stanton

The Journal of Chemical Physics ARTICLE scitation.org/journal/jcp

A master equation simulation for the •OH + CH_3OH reaction

Cite as: J. Chem. Phys. 150, 084105 (2019); doi: 10.1063/1.5081827
Submitted: 16 November 2018 • Accepted: 1 February 2019 •
Published Online: 25 February 2019

Thanh Lam Nguyen,[1] Branko Ruscic,[2] and John F. Stanton[1,a)]

AFFILIATIONS

[1]Quantum Theory Project, Department of Chemistry and Physics, University of Florida, Gainesville, Florida 32611, USA
[2]Chemical Sciences and Engineering Division, Argonne National Laboratory, 9700 South Cass Avenue, Argonne, Illinois 60439, USA

[a)]E-mail: johnstanton@ufl.edu

ABSTRACT

A combined (fixed-J) two-dimensional master-equation/semi-classical transition state theory/variational Rice-Ramsperger-Kassel-Marcus approach has been used to compute reaction rate coefficients of •OH with CH_3OH over a wide range of temperatures (10–2500 K) and pressures (10^{-1}–10^4 Torr) based on a potential energy surface that has been constructed using a modification of the high accuracy extrapolated *ab initio* thermochemistry (HEAT) protocol. The calculated results show that the title reaction is nearly pressure-independent when T > 250 K but depends strongly on pressure at lower temperatures. In addition, the preferred mechanism and rate constants are found to be very sensitive to temperature. The reaction pathway CH_3OH + •OH → CH_3O• + H_2O proceeds exclusively through tunneling at exceedingly low temperatures (T ≤ 50 K), typical of those established in interstellar environments. In this regime, the rate constant is found to increase with decreasing temperature, which agrees with low-temperature experimental results. The thermodynamically favored reaction pathway CH_3OH + •OH → •CH_2OH + H_2O becomes dominant at higher temperatures (T ≥ 200 K), such as those found in Earth's atmosphere as well as combustion environments. By adjusting the *ab initio* barrier heights slightly, experimental rate constants from 200 to 1250 K can be satisfactorily reproduced.

I. INTRODUCTION

The oxidation of methanol by a hydroxyl radical plays an important role in combustion, atmospheric, and interstellar chemistry[1–4] because this reaction is the most important sink for this simplest alcohol; it therefore determines the lifetime of CH_3OH in these environments. Because of its fundamental role, the title reaction has been studied extensively by both experiment[1–17] and theory.[18–21] It is believed to occur exclusively through hydrogen abstractions at the CH_3-group and the OH-group to produce two distinct products, viz., •CH_2OH and CH_3O•, respectively,

$$\text{•OH} + CH_3OH \rightarrow H_2O + \text{•}CH_2OH \quad \text{with} \quad \Delta H_{r1}(0\ \text{K}) = -96.62 \pm 0.32\ \text{kJ/mol}, \tag{1}$$

$$\text{•OH} + CH_3OH \rightarrow H_2O + CH_3O\text{•} \quad \text{with} \quad \Delta H_{r2}(0\ \text{K}) = -57.46 \pm 0.34\ \text{kJ/mol}. \tag{2}$$

Both reaction pathways are exothermic (as given above, based on to the recently published Active Thermochemical Tables (ATcT) values,[22] to be compared to the current mHEAT–*vide infra*–theoretical values of –96.78 and –57.15 kJ/mol, respectively) and have barriers. Pathway (1) is more exothermic and has a lower (theoretical) barrier height (by about 7.6 kJ/mol, see below) than pathway (2); the former is therefore predicted to be both kinetically and thermodynamically more favorable. Yet, channel (2) also becomes important when temperature increases, which has been well established.[2,19,20] Interestingly, in recent papers, Heard's group[2–4] as well as Antinolo *et al.*[17] have carried out experiments at very low temperatures, a characteristic of those in dense interstellar clouds; these authors have found that the measured rate constants increase significantly with decreasing temperature. At about 50 K, the observed rate constants are roughly *two orders of magnitude larger* than those at 200 K.[2,3,17] Additionally, only product channel (2) has been observed under these extremely

low temperature conditions. This finding is in contradiction to the usual expectation that a reaction with a barrier is not expected to play a role (or even to occur) at very low temperatures. Heard and co-workers then concluded that the title reaction at interstellar temperatures is enabled by quantum mechanical tunneling.[2–4] Such a tunneling controlled mechanism has also been observed for other reactions.[23,24] Furthermore, to support the experimental observation, Heard and co-workers[2] also did a chemical kinetic simulation using a one-dimensional master equation technique and the potential energy surface (PES) previously reported with CCSD(T)/6-311+G(3df,2p) level of theory.[19] These authors found that the calculated rate constant does indeed increase considerably as the temperature falls below 200 K, clearly validating the crucial role of tunneling. Yet, the calculated rate constants were about an order of magnitude smaller than the experimental values.[2]

Very recently, thermal rate constants (from 30 K to 2000 K) for the title reaction have been computed at the low- and high-pressure limits using a competitive canonical unified statistical (CCUS) model[20] where the quantum mechanical effects associated with barrier crossing are treated with a multi-structural torsional anharmonicity and small-curvature tunneling (MS-CVT/SCT) approach.[20] Potential energy surfaces (PESs) used for direct dynamics calculations were constructed with density functional theory (DFT) methods where energies of stationary points on the PES were examined against CCSD(T)-F12a/jun-cc-pVTZ and CASPT2/jun-cc-pVTZ calculations.[20] As shown in that paper, experimental results lie somewhere between the two extreme pressures in a low-temperature regime.[20] This computational result seems to imply that some fraction of energized van der Waals (vdW) complex of $^{\bullet}$OH and CH_3OH can be thermalized by collisions with bath gases, and then they tunnel through barriers to form products. In other words, it seems to suggest that the title reaction depends on pressure, at least in the low-temperature regime relevant to interstellar chemistry. In such a case, a master equation technique would be needed to obtain the associated falloff curve.

In this work, we use (fixed-J) two-dimensional master equation techniques[25–29] to compute thermal rate constants for an extensive range of temperature and pressure in order to better understand the kinetics and mechanism of the title reaction. We focus mainly on a very low-temperature regime (10–100 K) where the pressure-dependence of rate constant is more pronounced.

II. QUANTUM CHEMICAL CALCULATIONS

All key stationary points on the PES are characterized using high accuracy coupled-cluster calculations. First of all, geometries are fully optimized using coupled-cluster theory with single, double, and perturbative triple excitations (CCSD(T))[30,31] in combination with an atomic natural orbital triple-zeta (ANO1) basis set.[32,33] Harmonic vibrational analysis is then performed to verify the nature of the stationary points located: all real frequencies for a minimum and only one imaginary frequency for a transition state. Next, anharmonic corrections based on second-order vibrational perturbation theory (VPT2)[34] are calculated using CCSD(T) but with a smaller double-zeta (ANO0) basis set.[32,33] Finally, single-point energies are obtained using a composite method (denoted hereafter as mHEAT),[27,35] which is a slight modification of the original high accuracy extrapolated *ab initio* thermochemistry (HEAT) protocol[36–38] that makes it more applicable to medium-sized molecular systems. It has been shown that the mHEAT model[27,35] can yield an accuracy of better than 2 kJ/mol for relative energies (more detailed information can be found in the supplementary material).

Table I shows individual energies (relative to the initial reactants, $^{\bullet}$OH + CH_3OH) of various terms that compose the mHEAT energy. As seen in Table I, the three most important contributions arise from the SCF, CCSD(T), and zero-point vibrational energy (ZPE) calculations. SCF gives a good estimation for the binding energy of the vdW complex but significantly overestimates the barrier heights. For a transition state (TS), the CCSD(T) correction is very important, and it drops the barrier drastically. The ZPE difference is positive for the complex but negative for a TS, in part because the reaction coordinate motion in a TS is excluded. In addition, the higher-level correction including full triple and perturbative quadruple excitations is also important here for the TS; it lowers the barrier further (by ~2 kJ/mol). It should be noted that the spin-orbit correction of 0.46 kJ/mol,[38] from the experimental value for the $^{\bullet}$OH radical, is quite large in this case. The remaining contributions are small but collectively important.

Table II shows a comparison of mHEAT energies and those reported in the literature.[18,19] Barriers obtained in CCSD(T)/CBS calculations agree well (within 0.5 kJ/mol) with mHEAT, but both G2[18] and CCSD(T)/6-311+G(3df,2p)[19] levels of theory overshoot mHEAT by ~4 to 8 kJ/mol. The calculated thermal rate constants depend sensitively on a barrier height (especially at very low temperatures), so such differences assume importance. It is of interest to compare mHEAT (classical) barrier heights with those reported recently using CCSD(T)-F12a/jun-cc-pVTZ (see Table II).[20] Our classical barrier heights (e.g., excluding ZPE and the other small corrections) are 4.1 and 15.3 kJ/mol, respectively, for TS1 and TS2, which are about 2 kJ/mol lower than the values of 6.1 and 16.7 kJ/mol obtained by Gao *et al.*[20] Note that the higher-level correction (about −2 kJ/mol, see above) was not included in

TABLE I. Individual energies (kJ/mol) of various terms (relative to $^{\bullet}$OH + CH_3OH) calculated using the mHEAT-345(Q) method.

Individual term	Complex	TS1	TS2
δE(SCF → ∞)	−18.644	74.992	114.265
δE(CCSD(T) → ∞)	−7.837	−69.431	−96.614
δE(CCSDT)	0.019	−0.873	−0.915
δE(CCSDT(Q))	−0.076	−0.633	−1.443
δE(Core)	−0.151	0.002	−0.010
δE(DBOC)	0.022	0.070	0.294
δE(Scalar)	0.102	0.063	−0.076
δE(SO)	0.460	0.460	0.460
δE(ZPE)	7.831	−4.231	−7.930
Total mHEAT	−18.274	0.419	8.031

TABLE II. Comparison of relative energies (kJ/mol) of various stationary points in this work with those in the literature. The values given in parentheses are classical barrier heights, which exclude ZPE corrections.

Species	mHEAT[a]	CBS(aD, aT, aQ)[b]	Xu and Lin[c]	Jodkowski *et al.*[d]	Gao *et al.*[e]
OH + CH_3OH	0.00	0.00	0.00	0.00	0.00
Complex	−18.27 ± 2	−18.72	−20.50	n/a	n/a
TS1	0.42 ± 2 (4.1 ± 2)	0.27	4.18	3.77	(6.1)
TS2	8.03 ± 2 (15.3 ± 2)	8.62	15.90	14.64	(16.7)

[a]This work (see the main text).
[b]This work: total energies are calculated as CCSD(T)/CBS(aD,aT,aQ) + anharmonic ZPE + DBOC + scalar + SO + core + HLC.
[c]CCSD(T)/6-311+G(3df,2p)//MP2/6-311+G(3df,2p) level of theory.[19]
[d]G2 method.[18]
[e]Taken from Ref. 20.

the work of Gao *et al.*,[20] and this appears to be the principal reason for the difference in values. In this case, at least, CCSD(T) does not appear to "*be enough*."

III. CHEMICAL KINETICS CALCULATIONS

The schematic reaction energy profile is displayed in Fig. 1. The first step of the process is an association of •OH and CH_3OH to form a van der Waals complex, which has a binding energy of 18.3 kJ/mol. The fate of this complex, once produced, depends on the reaction conditions. Stabilization is highly unlikely at sufficiently high temperatures, but some of the complexes can be stabilized by collisions at lower temperatures. The remaining unstabilized complexes still have ample internal energy and can either re-dissociate back to the initial reactants or undergo an H-abstraction to produce •CH_2OH or CH_3O•. It should be mentioned that the stabilized complex can also subsequently decompose thermally to yield the same products, but the thermal decomposition process occurs on a time scale (much) longer than the chemically activated one. To better understand this complicated reaction process, a master equation approach must be used.

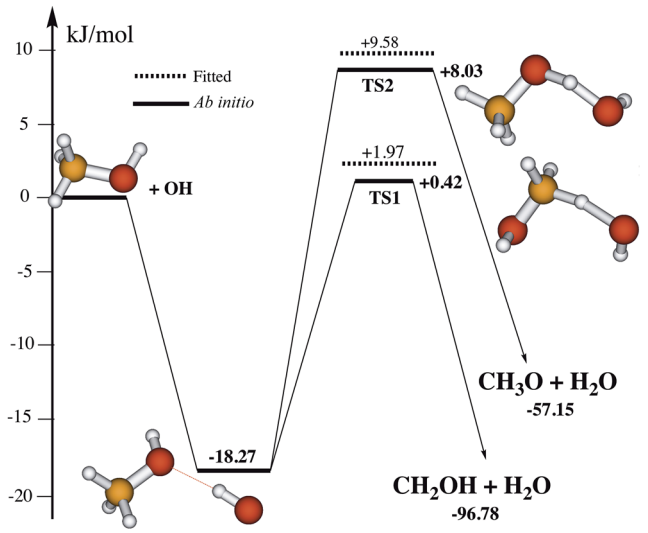

FIG. 1. Schematic reaction energy profile of •OH + CH_3OH reaction constructed using the mHEAT-345(Q) method: solid lines are current *ab initio* results; dotted lines display adjusted barrier heights.

A (fixed-J) two-dimensional master-equation (2DME)[39–43] that describes the time evolution of the complex, products, and reactants in the chemically activated reaction as displayed in Fig. 1 can be formulated as follows:

$$\frac{\partial C(E_m,J_m)}{\partial t} = \sum_{J_n=0}^{\infty}\int_{E_n=0}^{\infty} P(E_m,J_m|E_n,J_n)\cdot\omega\cdot C(E_n,J_n)\cdot dE_n - \omega\cdot C(E_m,J_m) - \{k_0(E_m,J_m)+k_1(E_m,J_m) + k_2(E_m,J_m)\}\cdot C(E_m,J_m) + k_\infty(T)\cdot F_{CA}(E_m,J_m)\cdot C_{OH}\cdot C_{CH_3OH}, \quad (3)$$

where ω (in s^{-1}) is the collision frequency, $C(E_m, J_m)$ is the population of complex at the internal energy E_m and the rotational angular quantum number J_m, C_{OH} and C_{CH3OH} are the concentrations of •OH and CH_3OH, $k_\infty(T)$ is the capture rate constant for the association of •OH and CH_3OH, which can be computed using (micro-variational) transition state theory at the high-pressure limit, $P(E_m,J_m|E_n,J_n)$ is the energy transfer probability function from an initial state (E_n, J_n) to a final state (E_m, J_m), and k_0, k_1, and k_2 are the microcanonical rate constants for the unimolecular dissociations of complex to •OH + CH_3OH, H_2O + •CH_2OH, and H_2O + CH_3O•, respectively. Because the reverse association of •OH and CH_3OH is a barrierless process, variational Rice-Ramsperger-Kassel-Marcus (vRRKM) theory[44–46] must be used to compute $k_0(E, J)$. The two H-abstraction pathways have tight TSs; thus, the semi-classical transition state theory (SCTST) approach[47–51] as implemented in the MULTIWELL program[52] can be employed to obtain $k_1(E, J)$ and $k_2(E, J)$. Note that hindered internal rotations having low vibrational frequencies in a TS that correspond to large-amplitude vibrations are projected out and treated (approximately) as separable one-dimensional hindered internal rotors (see the supplementary material). $F_{CA}(E_m, J_m)$ is the initial, nascent energy/angular momentum distribution function of the energized complex,

which is just formed from the association of •OH and CH_3OH and expressed as Eq. (4),[53–56]

$$F_{CA}(E,J) = \frac{(2J+1)k_0(E,J)\rho(E,J)\exp(-\frac{E}{RT})}{\sum_{J=0}^{\infty}\int_0^{\infty}(2J+1)k_0(E,J)\rho(E,J)\exp(-\frac{E}{RT})dE}. \quad (4)$$

Here $\rho(E, J)$ is the rovibrational density of states of complex.

To solve Eq. (3), in this work, we use a fixed-J model for the energy/angular momentum transition probability function. We assume that total internal energy can change through collisions, but total angular momentum (J) remains unchanged (i.e., J is fixed). Therefore, the $P(E_m, J_m|E_n, J_n)$ function can be simplified to a one-dimensional function, which now depends on a total internal energy only,

$$P(E_m, J_m|E_n, J_n) = P(E_m, J|E_n, J) = P(E_m|E_n)_J = P(E_m|E_n).$$

Advantages and drawbacks of this quite simple model have been discussed in our recent papers.[25–29]

A. Low-pressure limit, P = 0

The stabilized yield of complex is zero; thus, Eq. (3) has an analytical solution–total rate constant yielding products–given by Eq. (5),[24,57]

$$k_{Products}(T, P=0) = \frac{\sigma}{h}\cdot\{Q_t^{\neq}\cdot Q_e^{\neq}\} \cdot \frac{\sum_{J=0}^{\infty}(2J+1)\int_{E=0}^{\infty}\frac{(G_1^{\neq}(E,J)+G_2^{\neq}(E,J))\cdot G_0^{\neq}(E,J)\exp(-\frac{E}{RT})dE}{G_0^{\neq}(E,J)+G_1^{\neq}(E,J)+G_2^{\neq}(E,J)}}{Q_{OH}Q_{CH_3OH}}, \quad (5)$$

where σ = 2 is the reaction path degeneracy, both TSs being enantiomeric, $Q_t^{\neq}$ and $Q_e^{\neq}$ are the translational and electronic partition functions of a TS, R is the gas constant, h is Planck's constant, Q_{OH} and Q_{CH_3OH} are the complete partition functions of •OH and CH_3OH, respectively, and $G_i^{\neq}(E, J)$ is the rovibrational cumulative reaction probability through TSi.

The rovibronic coupling in OH plays an important role in the low temperature partition function of OH radical and must be explicitly considered here. In this work, the coupled electronic-rotational-vibrational partition function is obtained by a procedure for generating diatomic partition functions currently used in Active Thermochemical Tables (ATcT).[58–60] For OH, this involves a direct count over ~1150 bound rovibronic levels of the $X\,^2\Pi_i$ state, the energies, degeneracies, and quantum numbers of which were calculated from a slightly expanded set of known experimental spectroscopic constants using the Hill-Van Vleck Hamiltonian.[61,62] It should be mentioned that the uncoupled model using the usual assumption of separable rotational, vibrational, and electronic components to partition functions underestimates the correct partition function of OH: the ratio between the two is found to be 3.95 at 10 K, 2.03 at 50 K, and 1.49 at 100 K, dropping to 1.15 at 300 K and becoming only about 1.06 between 1000 and 2500 K. More detailed information can be found in the supplementary material.

B. High-pressure limit, P = ∞

First, the complex is completely stabilized by collisions. Then, it is rapidly re-populated thermally. The thermalized complex can subsequently decompose to give products, CH_3O• and •CH_2OH. Applying the steady-state approximation to the complex, a total rate constant forming the products can be computed via Eq. (6),

$$k_{Products}(T, P=\infty) = \frac{\{k_1(T)+k_2(T)\}\cdot k_\infty(T)}{k_0(T)+k_1(T)+k_2(T)} = \frac{\{Q_{TS1}+Q_{TS2}\}\cdot k_\infty(T)}{Q_{TS0}+Q_{TS1}+Q_{TS2}}. \quad (6)$$

Here, $k_i(T)$ is the rate constant for the (thermal) unimolecular dissociation of complex through TSi calculated at the high-pressure limit, and Q_{TSi} is the complete partition function of TSi.

As seen in Eqs. (5) and (6), rate constants calculated at the low- and high-pressure limits are apparently independent on rovibrational parameters of the complex. In particular, the low-P limit rate constants in this work–which are most relevant to applications in interstellar chemistry as well as to combustion where k(T) is pressure-independent–are wholly independent on the complex rovibrational parameters.

At other pressures in the falloff regime, one must solve Eq. (3) numerically to obtain product branching ratios (γ^{CA}). If the stabilized yield of complex is not negligibly small, one must solve a second master-equation for a thermally activated decomposition of complex to obtain product yields (γ^{TA}). Once completed, a total rate constant can be calculated using Eq. (7). More detailed solutions to the master equation are given in the supplementary material,

$$k_{Products}(T,P) = k_\infty(T)\cdot\left[\gamma_{CH_3O}^{CA}+\gamma_{CH_2OH}^{CA}+\gamma_{Complex}^{CA}\cdot\left(\gamma_{CH_3O}^{TA}+\gamma_{CH_2OH}^{TA}\right)\right], \quad (7)$$

where CA and TA stand for chemically activated and thermally activated systems, respectively. As shown in the supplementary material, Eqs. (5) and (6) are two simple limiting cases that can be derived from Eq. (7).

IV. RESULTS AND DISCUSSION

The calculated thermal rate constants depend sensitively on various factors including barrier height, tunneling correction, ro-vibrational parameters, and anharmonic constants. Of those, the barrier height is the most important parameter, which will be adjusted while the remaining parameters are fixed. For the reaction system considered here, it is very challenging to get accuracy better than 1 kJ/mol from quantum chemical calculations. For the purpose of doing a kinetics simulation in this work, we raised both calculated barrier heights by 1.55 kJ/mol (which still lies within a plausible error bar for the mHEAT method) in order to match the well-established experimental rate constant of (9.5 ± 0.5) × 10^{-13} cm^3 $molecule^{-1}$ s^{-1} at room temperature.[1] We then

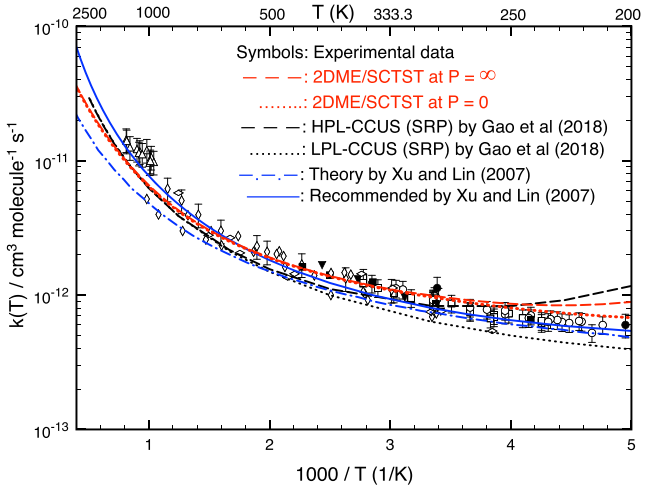

FIG. 2. Bimolecular rate constants calculated as functions of temperature (200-2500 K) and pressure using the 2DME/SCTST/VPT2+ approach. Other theoretical studies and experimental data are also included for comparison.

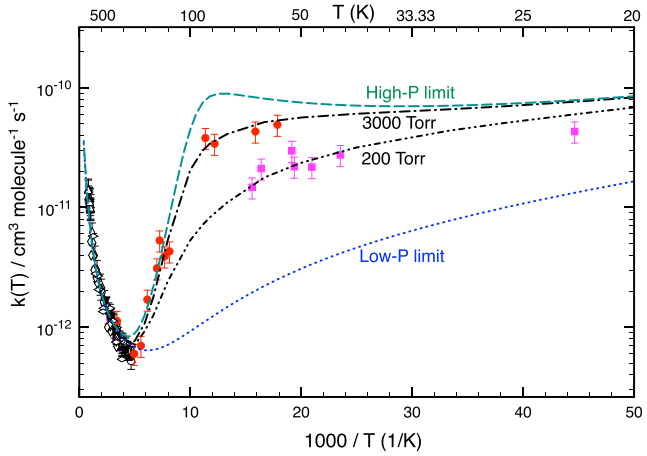

FIG. 4. Bimolecular rate constants calculated for an extensive temperature range of 20-2500 K and as a function of pressure using the 2DME/SCTST/VPT2+ approach. Symbols are experimental data: filled red circles from Refs. 2 and 3 with $P_{exptl.} < 2$ Torr; filled pink squares from Ref. 17 with $P_{exptl.} < 0.4$ Torr.

use these adjusted barriers to estimate rate constants at other temperatures.

Figure 2 shows rate constants calculated at two different pressures and T ≥ 200 K, which are relevant to atmospheric and combustion applications.[1,5–16,18–20] As seen, the calculated rate constants agree well with experimental results (within ~20%)[1] and are nearly pressure-independent when temperature is greater than 250 K. Below 250 K, the theoretical rate constants (slightly) depend on pressure, and experimental data available are clearly in the low-pressure regime. Figure 2 also reveals a comparison of this work with the two previous studies.[19,20] As compared to the benchmark experimental data, our results are very similar to those obtained previously and maintain relatively consistent accuracy for the whole temperature range 200-2500 K. Note that the modified Arrhenius curve recommended by Xu and Lin[19] also agrees nicely with the experimental results.

Figure 3 reveals that the calculated rate constants are strongly dependent on both pressure (10^{-1}–10^{4} Torr) and temperature (10–100 K) under conditions relevant to interstellar and circumstellar chemistry. Interestingly, the rate constants increase with pressure (as expected) but (surprisingly) decrease with rising temperature. In addition, the pressure-dependence at 10 K is less pronounced than at 100 K. This behavior is the result of two coupled effects: one is the increase in the stabilized yield of the complex when temperature decreases, and the other is the tunneling-controlled decomposition mechanism of the complex at very low temperatures, in accordance with experimental observation.[2,3,17] It is well-established that quantum mechanical tunneling strongly

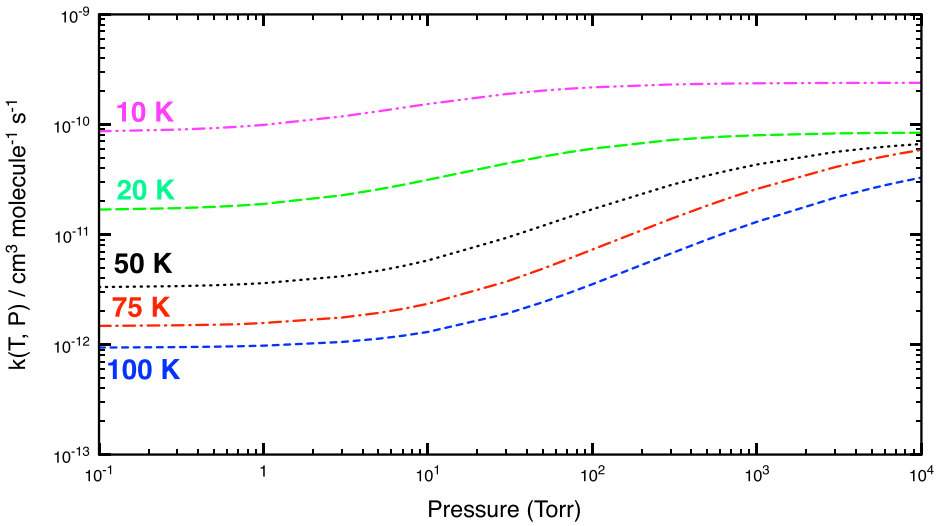

FIG. 3. Bimolecular rate constants calculated as a function of pressure (10^{-1}–10^{4} Torr) in an extremely low temperature regime (10-100 K) using the 2DME/SCTST/VPT2+ approach.

TABLE III. Comparison of thermal rate constants (cm^3 $molecule^{-1}$ s^{-1}) calculated at the low- and the high-pressure limits using 2DME/SCTST/VPT2+ and CCUS(SRP)[20] approaches.

T (K)	2DME/SCTST (P = 0)	LPL-CCUS (SRP)[a]	2DME/SCTST (P = ∞)	HPL-CCUS (SRP)[a]
30	7.72×10^{-12}	7.71×10^{-13}	7.06×10^{-11}	1.09×10^{-10}
35	5.90×10^{-12}	6.46×10^{-13}	6.99×10^{-11}	1.17×10^{-10}
40	4.62×10^{-12}	5.60×10^{-13}	7.08×10^{-11}	1.25×10^{-10}
45	3.74×10^{-12}	4.98×10^{-13}	7.26×10^{-11}	1.33×10^{-10}
50	3.08×10^{-12}	4.51×10^{-13}	7.51×10^{-11}	1.40×10^{-10}
63	2.10×10^{-12}	3.76×10^{-13}	8.26×10^{-11}	1.57×10^{-10}
70	1.67×10^{-12}	3.51×10^{-13}	8.70×10^{-11}	1.66×10^{-10}
80	1.32×10^{-12}	3.28×10^{-13}	8.89×10^{-11}	1.76×10^{-10}
90	1.08×10^{-12}	3.14×10^{-13}	7.46×10^{-11}	1.78×10^{-10}
100	9.24×10^{-13}	3.06×10^{-13}	4.46×10^{-11}	1.44×10^{-10}
110	8.16×10^{-13}	3.04×10^{-13}	2.15×10^{-11}	7.93×10^{-11}
120	7.42×10^{-13}	3.05×10^{-13}	1.04×10^{-11}	3.54×10^{-11}
125	7.16×10^{-13}	3.06×10^{-13}	7.46×10^{-12}	2.38×10^{-11}
130	6.94×10^{-13}	3.09×10^{-13}	5.51×10^{-12}	1.63×10^{-11}
135	6.77×10^{-13}	3.12×10^{-13}	4.19×10^{-12}	1.15×10^{-11}
150	6.47×10^{-13}	3.24×10^{-13}	2.17×10^{-12}	4.87×10^{-12}

[a]Taken from Table S8 of Ref. 20.

correlates with the magnitude of the reaction coordinate (imaginary) vibrational frequency, ω_F: a larger ω_F generates a thinner barrier, thus resulting in an enhanced tunneling probability. TS2 has an ω_F of 2017i, about 2.4 times larger than that of TS1 (ω_F = 836i). So, it is not entirely surprising that pathway 2 dominates at low temperatures, and that below 50 K, $CH_3O^\bullet$ becomes the sole product. At 10 K in cold, dense clouds, we estimate a rate constant varying from 0.9×10^{-10} cm^3 $molecule^{-1}$ s^{-1} at the zero-pressure to 2.4×10^{-10} cm^3 $molecule^{-1}$ s^{-1} at the high-pressure limit, which is in good agreement with values used in models from 0.4 to 3×10^{-10} cm^3 $molecule^{-1}$ s^{-1}.[4,17]

Figure 4 displays the rate constants calculated for an expanded range of temperatures and pressures. In the low temperature regime (20–250 K), the rate constants fall quickly with temperature and reach a minimum at about 200 K, beyond which the rate constants increase sharply with temperature. This result leads to a curious-looking curve for the temperature-dependence of the rate constant as has also been reported recently by others.[20] Inspection of Fig. 4 also shows that in the very low-temperature regime, the experimental results of Heard and co-workers[2,3] can be reproduced using a (higher) pressure of 3000 Torr, and the experimental results of Antinolo *et al.*[17] can be mimicked using a (lower) pressure of 200 Torr. These two working pressures are roughly two to three orders of magnitude higher than those actually used in the experiments.[2,3,17] An explanation for these differences is not readily apparent. It has been suggested that formation of dimers of CH_3OH at very low temperatures,[63] followed by their fast reactions with $^\bullet OH$ radicals, could lead to a larger overall reaction rate constant. However, this idea is not unanimously accepted.[64,65] It might also be speculated that the van der Waals complex of $^\bullet OH$ and CH_3OH has a short lifetime, thus not exhibiting statistical behavior.[66] Further studies are clearly warranted.

It is of interest to compare the 2DME/SCTST/VPT2+ results with those from Ref. 20 in a low temperature range (30-150 K, see Table III). As seen there, the results of both approaches agree well with each other (within 30%) for the high-pressure limit and temperatures below 35 K. However, at higher temperatures, there is a difference of a factor of 2–3. For the low-pressure limit, the agreement between two approaches is quite good; this is partly because of the difference in formulas used [the microcanonical model, Eq. (5), in this work versus the canonical model, Eq. (12), in Ref. 20].

V. CONCLUSIONS

In summary, (fixed-J) two-dimensional master equation methods are used to simulate the title reaction under extremely low temperatures relevant to interstellar chemistry. It is found that the rate constant increases significantly as temperature decreases as has previously been observed experimentally and computationally. A rate constant estimated at 10 K in cold, dense clouds of stars is 10^{-10} cm^3 $molecule^{-1}$ s^{-1}, approximately two orders of magnitude faster than that at room temperature. This remarkable result is due to the fact that the yield of the complex rises with lowering temperature and that tunneling controls its succeeding decomposition under these extremely low-temperature conditions.

SUPPLEMENTARY MATERIAL

See supplementary material for theoretical methods, additional results, optimized geometries, and rovibrational parameters, for various stationary points are provided.

ACKNOWLEDGMENTS

The work at the University of Florida (T.L.N. and J.F.S.) was supported by the U.S. Department of Energy, Office of

Science, Office of Basic Energy Sciences under Award No. DE-FG02-07ER15884 and the U.S. Air Force Office of Scientific Research (No. FA9550-16-1-0117). The work at the Argonne National Laboratory (B.R.) was supported by the U.S. Department of Energy, Office of Science, Office of Basic Energy Sciences, Division of Chemical Sciences, Geosciences and Biosciences under Contract No. DE-AC02-06CH11357. Aspects of this work at the University of Florida were also supported by the U.S. National Science Foundation, under Grant No. CHE-1748821. We would like to thank Professor Dwayne E. Heard, University of Leeds, and Professor John R. Barker, University of Michigan in Ann Arbor, for their helpful discussions. We would also like to express our gratitude to two anonymous reviewers for their useful comments that improved the quality of this paper.

REFERENCES

[1]D. L. Baulch, C. T. Bowman, C. J. Cobos, R. A. Cox, T. Just, J. A. Kerr, M. J. Pilling, D. Stocker, J. Troe, W. Tsang, R. W. Walker, and J. Warnatz, J. Phys. Chem. Ref. Data **34**, 757–1397 (2005).
[2]R. J. Shannon, M. A. Blitz, A. Goddard, and D. E. Heard, Nat. Chem. **5**, 745–749 (2013).
[3]J. C. G. Martin, R. L. Caravan, M. A. Blitz, D. E. Heard, and J. M. C. Plane, J. Phys. Chem. A **118**, 2693–2701 (2014).
[4]K. Acharyya, E. Herbst, R. L. Caravan, R. J. Shannon, M. A. Blitz, and D. E. Heard, Mol. Phys. **113**, 2243–2254 (2015).
[5]J. A. Mccaulley, N. Kelly, M. F. Golde, and F. Kaufman, J. Phys. Chem. **93**, 1014–1018 (1989).
[6]W. P. Hess and F. P. Tully, J. Phys. Chem. **93**, 1944–1947 (1989).
[7]E. Jimenez, M. K. Gilles, and A. R. Ravishankara, J. Photochem. Photobiol., A **157**, 237–245 (2003).
[8]U. Meier, H. H. Grotheer, and T. Just, Chem. Phys. Lett. **106**, 97–101 (1984).
[9]P. G. Greenhill and B. V. Ogrady, Aust. J. Chem. **39**, 1775–1787 (1986).
[10]T. J. Wallington and M. J. Kurylo, Int. J. Chem. Kinet. **19**, 1015–1023 (1987).
[11]J. Hagele, K. Lorenz, D. Rhasa, and R. Zellner, Ber. Bunsengesellschaft Phys. Chem. **87**, 1023–1026 (1983).
[12]T. J. Dillon, D. Holscher, V. Sivakumaran, A. Horowitz, and J. N. Crowley, Phys. Chem. Chem. Phys. **7**, 349–355 (2005).
[13]L. T. Zaczek, K. Y. Lam, D. F. Davidson, and R. K. Hanson, Proc. Combust. Inst. **35**, 377–384 (2015).
[14]A. Parker, C. Jain, C. Schoemaecker, and C. Fittschen, React. Kinet. Catal. Lett. **96**, 291–297 (2009).
[15]C. L. Rasmussen, K. H. Wassard, K. Dam-Johansen, and P. Glarborg, Int. J. Chem. Kinet. **40**, 423–441 (2008).
[16]K. L. Feilberg, M. Gruber-Stadler, M. S. Johnson, M. Muhlhauser, and C. J. Nielsen, J. Phys. Chem. A **112**, 11099–11114 (2008).
[17]M. Antinolo, M. Agundez, E. Jimenez, B. Ballesteros, A. Canosa, G. El Dib, J. Albaladejo, and J. Cernicharo, Astrophys. J. **823**, 25/1–25/8 (2016).
[18]J. T. Jodkowski, M. T. Rayez, J. C. Rayez, T. Berces, and S. Dobe, J. Phys. Chem. A **103**, 3750–3765 (1999).
[19]S. Xu and M. C. Lin, Proc. Combust. Inst. **31**, 159–166 (2007).
[20]L. G. Gao, J. J. Zheng, A. Fernandez-Ramos, D. G. Truhlar, and X. F. Xu, J. Am. Chem. Soc. **140**, 2906–2918 (2018).
[21]A. Galano, J. R. Alvarez-Idaboy, G. Bravo-Perez, and M. E. Ruiz-Santoyo, Phys. Chem. Chem. Phys. **4**, 4648–4662 (2002).
[22]B. Ruscic, J. Phys. Chem. A **119**, 7810–7837 (2015).
[23]P. R. Schreiner, H. P. Reisenauer, D. Ley, D. Gerbig, C. H. Wu, and W. D. Allen, Science **332**, 1300–1303 (2011).
[24]T. L. Nguyen, B. C. Xue, R. E. Weston, J. R. Barker, and J. F. Stanton, J. Phys. Chem. Lett. **3**, 1549–1553 (2012).
[25]T. L. Nguyen and J. F. Stanton, J. Phys. Chem. A **119**, 7627–7636 (2015).
[26]T. L. Nguyen, H. Lee, D. A. Matthews, M. C. McCarthy, and J. F. Stanton, J. Phys. Chem. A **119**, 5524–5533 (2015).
[27]T. L. Nguyen, L. McCaslin, M. C. McCarthy, and J. F. Stanton, J. Chem. Phys. **145**, 131102/1–131102/5 (2016).
[28]T. L. Nguyen, J. H. Thorpe, D. H. Bross, B. Ruscic, and J. F. Stanton, J. Phys. Chem. Lett. **9**, 2532–2538 (2018).
[29]T. L. Nguyen and J. F. Stanton, J. Phys. Chem. A **122**, 7757–7767 (2018).
[30]R. J. Bartlett, J. D. Watts, S. A. Kucharski, and J. Noga, Chem. Phys. Lett. **165**, 513–522 (1990).
[31]K. Raghavachari, G. W. Trucks, J. A. Pople, and M. Head-Gordon, Chem. Phys. Lett. **157**, 479–483 (1989).
[32]J. Almlof and P. R. Taylor, J. Chem. Phys. **86**, 4070–4077 (1987).
[33]J. Almlof and P. R. Taylor, J. Chem. Phys. **92**, 551–560 (1990).
[34]I. M. Mills, in *Molecular Spectroscopy: Modern Research*, edited by K. N. Rao and C. W. Mathews (Academic Press, New York, 1972), Vol. 1, pp. 115–140.
[35]T. L. Nguyen, B. C. Xue, G. B. Ellison, and J. F. Stanton, J. Phys. Chem. A **117**, 10997–11005 (2013).
[36]A. Tajti, P. G. Szalay, A. G. Csaszar, M. Kallay, J. Gauss, E. F. Valeev, B. A. Flowers, J. Vazquez, and J. F. Stanton, J. Chem. Phys. **121**, 11599–11613 (2004).
[37]Y. J. Bomble, J. Vazquez, M. Kallay, C. Michauk, P. G. Szalay, A. G. Csaszar, J. Gauss, and J. F. Stanton, J. Chem. Phys. **125**, 064108/1–064108/8 (2006).
[38]M. E. Harding, J. Vazquez, B. Ruscic, A. K. Wilson, J. Gauss, and J. F. Stanton, J. Chem. Phys. **128**, 114111/1–114111/15 (2008).
[39]S. J. Jeffery, K. E. Gates, and S. C. Smith, J. Phys. Chem. **100**, 7090–7096 (1996).
[40]S. H. Robertson, M. J. Pilling, K. E. Gates, and S. C. Smith, J. Comput. Chem. **18**, 1004–1010 (1997).
[41]J. A. Miller, S. J. Klippenstein, and C. Raffy, J. Phys. Chem. **106**, 4904–4913 (2002).
[42]A. W. Jasper, K. M. Pelzer, J. A. Miller, E. Kamarchik, L. B. Harding, and S. J. Klippenstein, Science **346**, 1212–1215 (2014).
[43]P. K. Venkatesh, A. M. Dean, M. H. Cohen, and R. W. Carr, J. Chem. Phys. **111**, 8313–8329 (1999).
[44]D. G. Truhlar and B. C. Garrett, Annu. Rev. Phys. Chem. **35**, 159–189 (1984).
[45]D. G. Truhlar, B. C. Garrett, and S. J. Klippenstein, J. Phys. Chem. **100**, 12771–12800 (1996).
[46]W. L. Hase, Acc. Chem. Res. **16**, 258–264 (1983).
[47]W. H. Miller, Faraday Discuss. **62**, 40–46 (1977).
[48]R. Hernandez and W. H. Miller, Chem. Phys. Lett. **214**, 129–136 (1993).
[49]T. L. Nguyen, J. F. Stanton, and J. R. Barker, Chem. Phys. Lett. **499**, 9–15 (2010).
[50]T. L. Nguyen, J. F. Stanton, and J. R. Barker, J. Phys. Chem. A **115**, 5118–5126 (2011).
[51]J. F. Stanton, J. Phys. Chem. Lett. **7**, 2708–2713 (2016).
[52]J. R. Barker, T. L. Nguyen, J. F. Stanton, C. Aieta, M. Ceotto, F. Gabas, T. J. D. Kumar, C. G. L. Li, L. L. Lohr, A. Maranzana, N. F. Ortiz, J. M. Preses, J. M. Simmie, J. A. Sonk, and P. J. Stimac, *MultiWell Program Suite*, Climate and Space Sciences and Engineering (University of Michigan, Ann Arbor, MI, 2017).
[53]W. Forst, *Theory of Unimolecular Reactions* (Academic Press, New York, 1973).
[54]W. Forst, *Unimolecular Reactions: A Concise Introduction* (Cambridge University Press, Cambridge, UK; New York, 2003).
[55]K. A. Holbrook, M. J. Pilling, S. H. Robertson, and P. J. Robinson, *Unimolecular Reactions*, 2nd ed. (Wiley, Chichester, New York, 1996).
[56]R. G. Gilbert and S. C. Smith, *Theory of Unimolecular and Recombination Reactions* (Blackwell Scientific Publications; Publishers' Business Services Distributor, Oxford; Boston, Brookline Village, Mass., 1990).
[57]W. H. Miller, J. Chem. Phys. **65**, 2216–2223 (1976).
[58]B. Ruscic, R. E. Pinzon, M. L. Morton, G. von Laszewski, S. J. Bittner, S. G. Nijsure, K. A. Amin, M. Minkoff, and A. F. Wagner, J. Phys. Chem. A **108**, 9979–9997 (2004).

[59]B. Ruscic, R. E. Pinzon, G. von Laszewski, D. Kodeboyina, A. Burcat, D. Leahy, D. Montoya, and A. F. Wagner, J. Phys. Conf. Ser. **16**, 561–570 (2005).
[60]B. Ruscic and D. H. Bross, Active Thermochemical Tables (ATcT) Values Based on Version 1.122d of the Thermochemical Network, 2018, available at ATcT.anl.gov.
[61]G. Herzberg, *Molecular Spectra and Molecular Structure. I. Spectra of Diatomic Molecules*, 2nd ed. (R.E. Krieger Pub. Co., Malabar, Fla., 1989).
[62]E. Hill and J. H. Van Vleck, Phys. Rev. **32**, 0250–0272 (1928).
[63]W. Siebrand, Z. Smedarchina, E. Martinez-Nunez, and A. Fernandez-Ramos, Phys. Chem. Chem. Phys. **18**, 22712–22718 (2016).
[64]W. Siebrand, Z. Smedarchina, D. Ferro-Costas, E. Martinez-Nunez, and A. Fernandez-Ramos, Phys. Chem. Chem. Phys. **20**, 8355–8357 (2018).
[65]R. J. Shannon, J. C. G. Martin, R. L. Caravan, M. A. Blitz, J. M. C. Plane, D. E. Heard, M. Antinolo, M. Agundez, E. Jimenez, B. Ballesteros, A. Canosa, G. El Dib, J. Albaladejo, and J. Cernicharo, Phys. Chem. Chem. Phys. **20**, 8349–8354 (2018).
[66]H. Guo, Int. Rev. Phys. Chem. **31**, 1–68 (2012).